Spatial correlations and Raman scattering interferences in self-assembled quantum dot multilayers

M. Cazayous, J. Groenen, J. R. Huntzinger, and A. Mlayah
Laboratoire de Physique des Solides, UMR 5477, Université P. Sabatier, 118 Route de Narbonne, 31062 Toulouse Cedex 4, France

O. G. Schmidt
Max Planck Institut für Festkörperforschung, Heisenbergstraβe 1, 70569 Stuttgart, Germany
(Received 9 March 2001; published 12 June 2001)

Raman scattering is shown to provide an effective means to measure spatial correlations in self-assembled quantum dot multilayers. Raman scattering interferences occur when an acoustic phonon interacts with an ensemble of localized electronic states. The interference contrast depends on their spatial correlations. Vertical correlations in self-assembled Ge/Si quantum dot multilayers are deduced from the interference contrast and successfully compared with those measured by transmission electron microscopy.

DOI: 10.1103/PhysRevB.64.033306 PACS number(s): 78.30.−j, 63.20.Kr, 81.07.Ta, 81.15.Hi

I. INTRODUCTION

Self-organization within semiconductor quantum dot (QD) ensembles has received much attention recently. In particular, long range ordering has been reported for self-assembled QD multilayers.[1–5] These QD's self-assemble during growth of lattice mismatched layers, providing effective strain relief. When QD layers are stacked, the burried dots influence the nucleation in the subsequent layers. This interaction occurs via elastic strain fields and induces vertical QD alignment.[1–3] It may lead to lateral ordering and size homogenization as well;[3,4] depending on the elastic anisotropy of the materials, various stacking sequences can be obtained.[4,5] Obviously, this self-organization offers interesting engineering possibilities. For instance, coupling between spatially correlated QD's provides a means of tuning electronic properties.[6] Taming this self-organization is thus a challenging goal. At this stage, modeling and experiments that allow a better understanding or provide reliable investigation tools are thus particularly valuable.

It is the purpose of this paper to show that QD spatial correlations can be addressed by resonant Raman scattering. Due to the lack of translational invariance in low dimensional systems, i.e., those involving localized electronic states, acoustic phonons are Raman active. The coupling between an acoustic phonon and a localized electronic state yields a continuous emission in the low frequency Raman spectrum, which is related to the Fourier transform of the electronic density.[7,8] Raman scattering interferences are expected if an acoustic phonon is likely to couple to an ensemble of localized electronic states. We recently observed such interferences in double stacks of self-assembled Ge/Si QD's.[9] These interferences were shown to depend in particular on the spacing between the QD layers. Here, we investigate how these interferences depend on the QD positions within the layers. We show that the interference contrast depends, in a systematic fashion, on the spatial correlation of the QD's.

II. MODEL

Let us consider identical quantum disks distributed within a multilayer structure. $\varphi_{n,l_p}(z)$ and $\psi_{m,l_p}(\vec{r})$ are wave functions that account for the confinement of the state (n,m) along the growth direction (z) and in plane $(\vec{r})$, respectively; p is the layer index and l_p is the QD index within layer p. Due to the lack of translation invariance, the usual wave vector conservation law does not hold here: all acoustic phonons may contribute to the Raman scattering. We consider the deformation potential interaction between a given acoustic phonon (wave vector $\vec{q}$ and displacement $\vec{u}_q$) and the ensemble of localized electronic states. We calculate the coherent superposition of all the scattering amplitudes. When double-resonance conditions with the states (n,m) and (n',m') are fullfilled, the Stokes Raman intensity is proportional to[10,11]

$$\left| \sum_{p,l_p} \vec{q}\cdot\vec{u}_q \int \psi^*_{m,l_p}(\vec{r}) e^{i(\Delta\vec{k}_{||}-\vec{q}_{||})\cdot\vec{r}} \psi_{m',l_p}(\vec{r}) d^2r \times \int \varphi^*_{n,l_p}(z) e^{i(\Delta k_z - q_z)z} \varphi_{n',l_p}(z) dz \right|^2 . \quad (1)$$

Δk_z $(\Delta\vec{k}_{||})$ is the difference between the incident and scattered photon wave vectors along (perpendicular to) the growth axis. The $\vec{q}$ nonconservation finds expression in both integrals. Because of the three-dimensional (3D) confinement neither q_z nor $q_{||}$ is conserved. Notice that if totally delocalized electronic states are considered one recovers the usual wave vector conservation law.

The coherent superposition of the QD scattering amplitudes yields interferences. These interferences depend on the electronic confinement within the QD (form factor) and on the relative QD positions (structure factor).

(i) The form factor determines the spectral envelope of the Raman scattering interferences. This envelope is related to the Fourier transform of the joint electronic densities $\varphi^*_{n,l_p}(z)\varphi_{n',l_p}(z)$ and $\psi^*_{m,l_p}(\vec{r})\psi_{m',l_p}(\vec{r})$.[7–9]

(ii) The structure factor determines the interference oscillation period and contrast. Since we have considered $\varphi_{n,l_p}(z)=\varphi_n(z-z_p)$ and $\psi_{m,l_p}(\vec{r})=\psi_m(\vec{r}-\vec{r}_{l_p})$ the Raman intensity is proportional to

$$\sum_{p} S_{pp}(\vec{q}_{||}) + 2\,\mathrm{Re}\left(\sum_{p \neq p'} e^{iq_z(z_p - z_{p'})} S_{pp'}(\vec{q}_{||}) \right), \qquad (2)$$

where

$$S_{pp'}(\vec{q}_{||}) = \sum_{l_p, l'_{p'}} e^{i\vec{q}_{||}\cdot(\vec{r}_{l_p} - \vec{r}_{l'_{p'}})}. \qquad (3)$$

$S_{pp}(\vec{q}_{||})$ and $S_{pp'}(\vec{q}_{||})$ are spatial correlation factors between electronic states within layer p and between layers p and p', respectively. The electronic state location (QD position) is given by z_p and $\vec{r}_{l_p}$ along the growth direction and in plane, respectively. Regularly spaced QD's (in plane or along the growth axis) should yield oscillations in the low frequency Raman signal. In particular, the spatial correlations should determine the interference contrast. We shall now demontrate that resonant Raman scattering indeed allows one to investigate spatial correlations in QD multilayers.

III. EXPERIMENTS AND SIMULATIONS

We investigate a series of Ge/Si self-assembled QD multilayers grown by molecular beam epitaxy on Si(001). Each multilayer contains five Ge QD layers. Five samples (hereafter labeled *A*, *B*, *C*, *D*, and *E*) with different Si interlayer thickness t (12.5, 25, 50, 75, and 100 nm, respectively) were grown. A 100 nm Si cap layer was deposited on the top of the multilayer. The QD's have the shape of planoconvex lenses with a mean height $h \simeq 6$ nm and base diameter $w \simeq 85$ nm. Notice that the samples investigated here belong to the series presented in Ref. 12.

Raman scattering was performed in backscattering geometry at room temperature in vacuum in order to avoid air related Raman peaks. The scattered light was detected by a T800 Coderg triple spectrometer coupled to a cooled photomultiplier. Spectra were excited with the 514 nm line of an Ar^+ laser in resonance with the E_1 transition of the QD's. According to optical phonon Raman spectra, the actual Ge content in the QD is about 70%.

Due to the large effective masses around the L point, the E_1 confinement induced energy shifts are negligible.[13] The spacings between E_1 sublevels are therefore very small with respect to the homogeneous broadening. This implies that (i) no particular quantum states can be selected via resonance; and (ii) owing to the small acoustic phonon energies, both incoming and outgoing resonance conditions (double resonance) can be easily fullfilled. Moreover, the inhomogenous broadening due to size fluctuations is expected to be much smaller than the homogenous broadening. We may therefore assume that all QD's have the same resonance factor. It is worth noting that no changes are observed in the spectral shapes of the Raman spectra when tuning the excitation energy around the E_1 transition.[9]

We performed three-dimensional simulations [Eq. (1)], considering different QD spatial distributions. Finite sampling effects were avoided by summing spectra calculated for many QD distributions. Simulations were performed with a

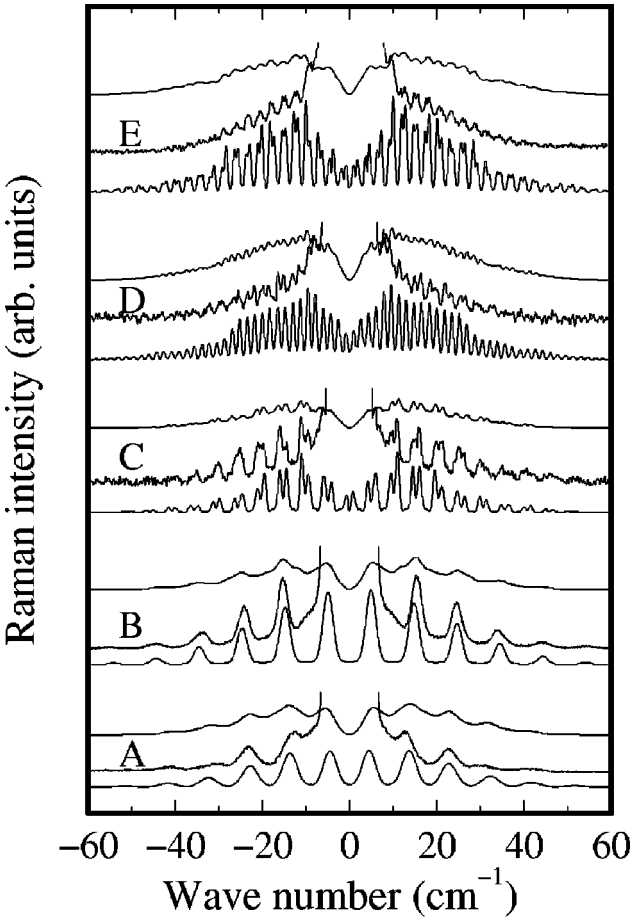

FIG. 1. Low frequency Raman spectra of samples *A*, *B*, *C*, *D*, and *E*. For each sample, three spectra are displayed: the one in the middle is the experimental one; the lower and the upper ones were calculated with vertically correlated QD and random QD distributions, respectively.

4×10^9 cm^{-2} QD density. In order to account for the finite spectral resolution, the results of calculations were convoluted with the spectral response of the experimental setup. As we are interested in QD spatial correlations (i.e., the structure factor), we shall adopt the following simple model for the electronic confinement (i.e., the form factor). The 3D QD's are modeled by quantum disks, with $\varphi_n(z)$ being a cosine function ($n=1$, first confined state) and $\psi_m(\vec{r})$ Bessel functions. Confinement determines the phonons that may contribute to the Raman signal. The more the electronic state is localized along a given direction, the more wave vector components along this direction do contribute. Here, the QD diameter is about one order of magnitude larger than its height. Hence, the phonons giving a significant contribution do have small in-plane wave vector components $q_{||}$. Their wave vector orientation is thus close to the growth axis. We shall therefore consider pure longitudinal acoustic modes with isotropic dispersion. We describe the lattice displacement of a given mode in each layer as the sum of counterpropagating plane waves. Their amplitudes have been obtained by considering displacement and stress field continuity at layer interfaces and a free sample surface.

IV. RESULTS AND DISCUSSION

Figure 1 presents low frequency Raman spectra recorded on samples *A*, *B*, *C*, *D*, and *E* (a Si reference spectrum has been subtracted). *A* and *B* spectra were obtained with a resolution of 2 cm^{-1}; *C*, *D*, and *E* spectra were recorded with 1.2 cm^{-1} resolution in order to resolve fine structures. Together with each experimental spectrum, spectra calculated using Eq. (1) are presented. The lower curves were calculated considering perfect vertically correlated island distributions (QD's have identical positions within the five layers, no in-plane ordering) whereas the upper calculated spectra were simulated with random QD distributions in all layers.

The periodic oscillations we observe in the low frequency Raman signals are due to the interferences discussed above. The oscillation period depends on the interlayer spacing *t* and the sound velocities (the latter were taken from Ref. 14); it decreases when *t* increases. The calculations account well for the periods observed experimentally. They also account for the width of the peaks. Increasing the number of layers results in sharper peaks (as expected for any kind of interference phenomenon). Here, the peaks are indeed much sharper than those reported for double stacks.[9] Spectra of samples *C*, *D*, and *E* display doublet peaks. According to the simulations, these fine structures originate from acoustic wave reflections. We emphasize that neither the observed peaks nor the doublets are related to zone folding effects. Increasing the number of layers results in accumulations in the phonon density of states and gap opening.[15,16] Here, the number of layers is small ($N=5$) and no gaps are opened in the acoustic phonon dispersion.

Calculations account rather well for the interference envelope. As mentioned above, the envelope depends on the electronic state dimensions. From the envelopes we deduced a decrease of the island mean height from 6 nm to 5 nm when the Si spacing increases from 12.5 nm to 100 nm. The elastic interaction between layers modifies the QD heights during the stacking process. For thin spacing this interaction is strong and results in an increasing island height. This increase does not occur for thick spacings, resulting in a lower mean height. Because the electronic wave function along the growth axis is more localized than its in-plane component, the Raman scattering interference envelope is more sensitive to height changes than width changes. It is therefore not obvious how to track QD width changes occurring during the stacking process (the width increases in the first two layers and stabilizes in the next ones[17,18]).

Let us now discuss the interference contrast. According to Eqs. (1) and (2), it depends greatly on the spatial distribution of the QD's. As we considered QD distributions without in-plane ordering within a given layer the QD's (S_{pp} structure factors) do not provide constructive interferences. The oscillating Raman scattering is therefore related to the spatial correlation factors $S_{pp'}$ between layers. For a given interlayer spacing, the interference contrast decreases when the spatial correlation between layers decreases. Whereas perfectly correlated QD's yield strong contrasts, randomly distributed ones display weak oscillations (Fig. 1). The amount of QD's that do interfere constructively depends on the spatial correlation. When no specific phase relationship exists the interferences blur. Interference contrast and interlayer spatial correlation are thus closely related. It is noteworthy that the residual contrast calculated for randomly distributed QD's depends on the average in-plane separations and diameters of the QD's [i.e., $\vec{r}_{l_p}-\vec{r}_{l'_{p'}}$ and $q_{||}$ in Eq. (3), respectively]. Here we find $\simeq 8\%$ residual contrast (Fig. 1), whatever the spacing of layers. For low QD densities this residual contrast vanishes.

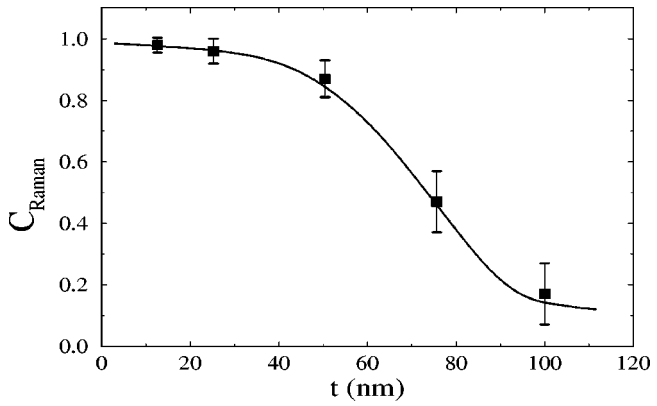

FIG. 2. Raman scattering interference contrast as a function of the Si interlayer thickness *t*. The solid line is a guide to the eye.

Figure 1 clearly shows that, experimentally, the interference contrast decreases when the interlayer thickness *t* increases. On one hand the spectra of samples *A*, *B*, and *C* are similar to the ones calculated with vertically correlated QD's. On the other hand the spectra of samples *D* and *E* are rather similar to the ones calculated with random QD distributions.

In order to quantify how the contrast depends on *t*, we define the following normalized Raman interference contrast: $C_{Raman}=(C^{exp}-C^{ran})/(C^{cor}-C^{ran})$ where C^{exp} is the experimental contrast, C^{ran} the contrast calculated with random QD distribution, and C^{cor} the contrast calculated with vertically correlated QD's. For a given spectrum (either

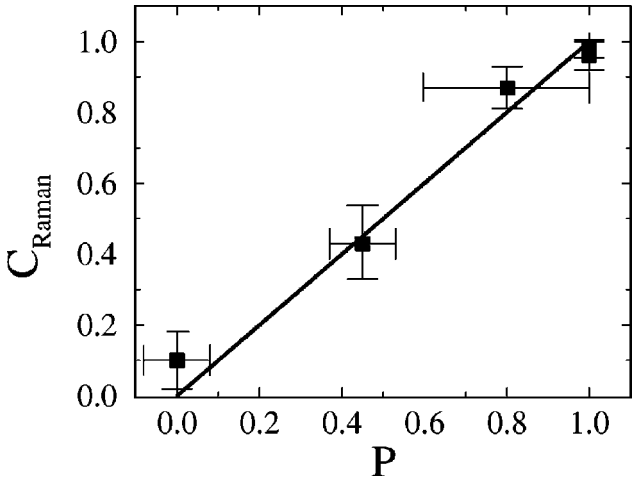

FIG. 3. Raman scattering interference contrast vs the degree of QD alignment *P* measured by TEM.

experimental or calculated) the first oscillations provide an almost constant value. The latter was used to compute C_{Raman}. According to the discussion just above, C_{Raman} provides a means of measuring spatial correlations. Perfect vertical correlation yields $C_{Raman}=1$ whereas a random distribution gives $C_{Raman}=0$. In Fig. 2 C_{Raman} is reported as a function of the interlayer spacing. Clearly $C_{Raman}\rightarrow 1$ for short spacings and $C_{Raman}\rightarrow 0$ for larger ones; C_{Raman} undergoes a rather steep transition for $t\approx 60$ nm. Note that if the QD distributions were random in the samples C_{Raman} would be equal to zero. Strikingly, this behavior is similar to the one reported for the QD alignment degree P measured by transmission electron microscopy (TEM).[12] It is interesting to compare quantitatively C_{Raman} and P for the different interlayer spacings. Indeed, Fig. 3 shows that the Raman interference contrast and TEM provide equivalent informations concerning the QD ordering. Thus, Fig. 3 corroborates that the Raman interference contrast allows one to quantify, in a reliable way, the vertical correlation of the QD's.

We have performed simulations including size fluctuations. As expected the latter reduce the interference contrast. For example the contrast changes resulting from fluctuations up to 15% remain within the vertical bars in Figs. 2 and 3. Anyway, despite all possible differences between QD's (size, composition, strain, etc.) we observe for thin spacings an experimental contrast as strong as the one calculated with correlated QD's.

V. CONCLUSION

In conclusion, we have shown, by both modeling and experiment, that Raman scattering provides an effective means of investigating spatial correlations between localized electronic states. It was shown that the interaction between acoustic phonons and an ensemble of QD's yields Raman scattering interferences. Simulations, including 3D electronic confinement and QD distributions, were performed in order to quantify how the interference contrast depends on the QD ordering. The vertical correlation in Ge/Si QD multilayers was derived from the Raman scattering interferences and successfully compared to the QD alignment deduced from TEM. It is thus demonstrated that Raman scattering by acoustic phonons is an efficient tool for investigating ordering within QD ensembles. Here we investigated vertical correlations. However, the Raman scattering interferences do depend on 3D spatial distributions. We therefore expect these interferences to allow the investigation of in-plane ordering as well.[3–5,19] We emphasize that these Raman scattering interferences provide 3D sampling and are relevant for investigating ordering over length scales ranging from a few to a few hundreds of nanometers.

[1] Q. Xie, A. Madhukar, P. Chen, and N.P. Kobayashi, Phys. Rev. Lett. **75**, 2542 (1995).

[2] G.S. Solomon, J.A. Trezza, A.F. Marshall, and J.S. Harris, Phys. Rev. Lett. **76**, 952 (1996).

[3] J. Tersoff, C. Teichert, and M.G. Lagally, Phys. Rev. Lett. **76**, 1675 (1996); C. Teichert, M.G. Lagally, L.J. Peticolas, J.C. Bean, and J. Tersoff, Phys. Rev. B **53**, 16 334 (1996).

[4] V. Holy, G. Springholz, M. Pinczolits, and G. Bauer, Phys. Rev. Lett. **83**, 356 (1999).

[5] G. Springholz, M. Pinczolits, P. Mayer, V. Holy, G. Bauer, H.H. Kang, and L. Salamanca-Riba, Phys. Rev. Lett. **84**, 4669 (2000).

[6] M. Colocci, A. Vinattieri, L. Lippi, F. Bogani, M. Rosa-clot, S. Taddei, A. Bosacchi, S. Franchi, and K. Ploog, Appl. Phys. Lett. **74**, 564 (1999).

[7] V.F. Sapega, V.I. Belitsky, A.J. Shields, T. Ruf, M. Cardona, and K. Ploog, Solid State Commun. **84**, 1039 (1992).

[8] A. Mlayah, A. Sayai, R. Grac, A. Zwick, R. Carles, M.A. Maaref, and R. Planel, Phys. Rev. B **56**, 1486 (1997).

[9] M. Cazayous, J.R. Huntzinger, J. Groenen, A. Mlayah, S. Christiansen, H.P. Strunk, O.G. Schmidt, and K. Eberl, Phys. Rev. B **62**, 7243 (2000).

[10] V.I. Belitsky, T. Ruf, J. Spitzer, and M. Cardona, Phys. Rev. B **49**, 8263 (1994).

[11] T. Ruf, J. Spitzer, V.F. Sapega, V.I. Belitsky, and M. Cardona, Phys. Rev. B **50**, 1792 (1994).

[12] O. Kienzle, F. Ernst, M. Rühle, O.G. Schmidt, and K. Eberl, Appl. Phys. Lett. **74**, 269 (1999).

[13] T.P. Pearsall, F.H. Pollak, J.C. Bean, and R. Hull, Phys. Rev. B **33**, 6821 (1986).

[14] M.H. Kuok, S.C. Ng, Z.L. Rang, and D.J. Lockwood, Phys. Rev. B **62**, 12 902 (2000).

[15] M.W.C. Dharma-Wardana, P.X. Zhang, and D.J. Lockwood, Phys. Rev. B **48**, 11 960 (1993).

[16] O. Pilla, V. Lemos, and M. Montagna, Phys. Rev. B **50**, 11 845 (1994).

[17] V. Le Thanh, V. Yam, P. Boucaud, F. Fortuna, C. Ulysse, D. Bouchier, L. Vervoort, and J.-M. Lourtioz, Phys. Rev. B **60**, 5851 (1999).

[18] O.G. Schmidt and K. Eberl, Phys. Rev. B **61**, 13 721 (2000).

[19] O.G. Schmidt, N.Y. Jin-Phillipp, C. Lange, U. Denker, K. Eberl, R. Schreiner, H. Gräbeldinger, and H. Schweizer, Appl. Phys. Lett. **77**, 4139 (2000).